NATIONAL ADVISORY COMMITTEE FOR AERONAUTICS

TECHNICAL NOTE 2078

HORIZONTAL TAIL LOADS IN MANEUVERING FLIGHT

By Henry A. Pearson, William A. McGowan, and James J. Donegan

Langley Aeronautical Laboratory
Langley Air Force Base, Va.

Washington
April 1950

NATIONAL ADVISORY COMMITTEE FOR AERONAUTICS

TECHNICAL NOTE 2078

HORIZONTAL TAIL LOADS IN MANEUVERING FLIGHT

By Henry A. Pearson, William A. McGowan,
and James J. Donegan

SUMMARY

A method is given for determining the horizontal tail loads in maneuvering flight. The method is based upon the assignment of a load-factor variation with time and the determination of a minimum time to reach peak load factor. The tail load is separated into various components. Examination of these components indicated that one of the components was so small that it could be neglected for most conventional airplanes, thereby reducing to a minimum the number of aerodynamic parameters needed in this computation of tail loads.

In order to illustrate the method, as well as to show the effect of the main variables, a number of examples are given.

Some discussion is given regarding the determination of maximum tail loads, maximum pitching accelerations, and maximum pitching velocities obtainable.

INTRODUCTION

The subject of maneuvering tail loads has received considerable attention both experimentally and theoretically. Theoretically, methods and solutions have been derived for determining the horizontal tail load following either a prescribed elevator motion (references 1 to 3) or an assigned load-factor variation (reference 4).

The first approach has been adopted into some of the load requirements where the type of elevator movement specified consists of linear segments whose magnitudes and rates of movement are governed by the assignment of a maximum initial elevator movement consistent with the pilot's strength. The rates of movement and the time the elevator is held before reversing are so adjusted that the design load factor will not be exceeded.

The results of reference 5 show, as is to be expected, that only when the aerodynamic force coefficients are accurately known from wind-tunnel tests can good agreement be obtained between measured and calculated tail loads. At the design stage, however, only general aerodynamic and geometric quantities are available and some of the more important stability parameters are not known accurately. Thus, the work involved in the solution for the tail load following a given elevator motion is not considered to be in keeping with the accuracy of the results obtained. Consequently, there appears to be a need for an abbreviated design method of computing tail loads which, although incorporating approximations, will nevertheless be based on the theoretical considerations of the problem.

If the load-factor variation with time is specified and the corresponding tail load, elevator angles, and load distributions are subsequently determined, a simpler and equally rational approach to the tail-load problem can be made. Although this approach has been used to a limited degree (reference 4), several shortcomings have limited its use.

The purpose of this paper is to develop further the load-factor or inverse approach and to present a method of computing horizontal tail loads which is comprehensive and generally simple. To this end, (1) the shape of the load-factor curve and the minimum time required to reach the peak load factor have been determined from an analysis of pull-up maneuvers that were available, (2) the minimum time required to reach the peak load factor has been determined from a theoretical analysis which is supported in some measure by statistical data obtained from a number of flight tests with airplanes of widely varying sizes, and (3) the equations relating the various quantities are presented.

SYMBOLS

b	wing span, feet; also shape factor in equation (13)
b_t	tail span, feet
c	chord, feet
$\bar{c}$	mean aerodynamic wing chord, feet
C_L	lift coefficient (L/qS)
C_m	pitching-moment coefficient of airplane without horizontal tail (Mb/qS^2)

C_{m_t}	pitching-moment coefficient of isolated horizontal-tail surface
g	acceleration of gravity, feet per second per second
I	pitching moment of inertia, slug-feet^2
k_Y	radius of gyration about pitching axis, feet
K	empirical constant denoting ratio of damping moment of complete airplane to damping moment of tail alone
L	lift, pounds
l	local lift at any spanwise station
m	airplane mass, slugs (W/g)
M	moment, foot-pounds
n	airplane load factor at any instant
N	maximum increment in load factor
q	dynamic pressure, pounds per square foot $\left(\frac{1}{2}\rho V^2\right)$
S	wing area, square feet
S_t	horizontal-tail area, square feet
t	time, seconds
t_1	time to reach peak of elevator deflection, seconds
V	airplane true velocity, feet per second
W	airplane weight, pounds
x_t	length from center of gravity of airplane to aerodynamic center of tail (positive for conventional airplanes), feet
y*	nondimensional spanwise dimension $\left(\frac{y}{b/2}\right)$

a,b,c A,B,C,D,E	constants occurring in equations (13), (23), (26), and (30)
K_1,K_2,K_3	constants occurring in basic differential equation (see equation (3) and table I)
λ	time to reach peak load factor, seconds
ρ	mass density of air, slugs per cubic foot
η_t	tail efficiency factor (q_t/q)
α	wing angle of attack, radians
$\bar{\alpha}$	average angle of attack of horizontal stabilizer, radians
α_t	tail angle of attack, radians
β	angle of sideslip, degrees
γ	flight-path angle, radians
θ	attitude angle, radians ($\alpha + \gamma$)
δ	elevator angle, radians
ϵ	downwash angle, radians $\left(\frac{d\epsilon}{d\alpha}\alpha\right)$
i_t	tail setting, radians

The notations $\dot{\alpha}$ and $\dot{\theta}$, $\ddot{\alpha}$ and $\ddot{\theta}$, and so forth, denote single and double differentiations with respect to t.

Subscripts:

o	initial or selected value
t	tail
max	maximum value
l_o	zero lift
geo	geometric
c	camber

METHODS

Method of Determining the Dynamic Tail Load

Basic equations of motion.— The simple differential equations for the longitudinal motion of an airplane for any elevator deflection (see method given in reference 2) may be written as

$$m\dot{\gamma}V - \frac{dC_L}{d\alpha}\Delta\alpha\, qS - \left(\frac{dC_L}{d\delta}\right)_t \eta_t qS_t\, \Delta\delta = 0 \tag{1}$$

$$\frac{dC_m}{d\alpha}\Delta\alpha q\frac{S^2}{b} - \Delta L_t x_t + \frac{dC_{m_t}}{d\delta}\eta_t q\frac{S_t^2}{b_t}\Delta\delta - mk_Y^2\,\ddot{\theta} = 0 \tag{2}$$

Equations (1) and (2) represent summations of forces perpendicular to the relative wind and of moments about the center of gravity. (See fig. 1 for direction of positive quantities.) Implicit in these equations are the following assumptions:

(1) In the interval between the start of the maneuver and the attainment of maximum loads, the flight-path angle does not change materially; therefore, the change in load factor due to flight-path change is small.

(2) At the Mach number for which computations are made, the aerodynamic derivatives are linear with angle of attack and elevator angle.

(3) The variation of speed during the maneuver may be neglected.

(4) Unsteady lift effects may be neglected.

By use of the relations $\theta = \gamma + \alpha$, $\dot{\theta} = \dot{\gamma} + \dot{\alpha}$, and $\ddot{\theta} = \ddot{\gamma} + \ddot{\alpha}$, equations (1) and (2) are reducible to the equivalent second-order differential equation

$$\ddot{\alpha} + K_1\dot{\alpha} + K_2\,\Delta\alpha = K_3\,\Delta\delta \tag{3}$$

where K_1, K_2, and K_3 are constants for a given set of conditions (see table I).

In equations (1) and (2), $\Delta\alpha$, $\dot{\gamma}$, $\ddot{\theta}$, $\Delta\delta$, and ΔL_t will, in a given maneuver, vary with time. Using the relations between θ, γ, α, and their derivatives permits equation (2) to be rewritten as follows to give the increment in tail load:

$$\Delta L_t = \frac{dC_m}{d\alpha}\Delta\alpha q \frac{S^2}{bx_t} - \frac{mk_Y^2\ddot{\alpha}}{x_t} - \frac{mk_Y^2\ddot{\gamma}}{x_t} + \frac{dC_{m_t}}{d\delta}\eta_t q \frac{S_t^2}{b_t x_t}\Delta\delta \qquad (4)$$

In a still shorter form, equation (4) may be written as

$$\Delta L_t = \Delta L_{t_\alpha} + \Delta L_{t_{\ddot{\alpha}}} + \Delta L_{t_{\ddot{\gamma}}} + \Delta L_{t_c} \qquad (5)$$

Equations (4) and (5) show that the tail-load increment (the increment above the steady-flight datum value) at any time is composed of four parts: ΔL_{t_α}, associated with the angle-of-attack change; $\Delta L_{t_{\ddot{\alpha}}}$, associated with angular acceleration about the flight path; $\Delta L_{t_{\ddot{\gamma}}}$, associated with angular acceleration of the flight path; and ΔL_{t_c}, required to compensate for the moment introduced by change in camber of the horizontal-tail surface. The load ΔL_{t_c} is generally small but in some extreme configurations may amount to 10 percent of the total increment and thus for the present it is retained in the development.

If the load-factor-increment variation with time Δn is known, then by the usual definition

$$\Delta n = \frac{dC_L}{d\alpha}\Delta\alpha\frac{q}{W/S} \qquad (6)$$

so that

$$\Delta\alpha = \frac{\Delta n\, W/S}{\frac{dC_L}{d\alpha} q}$$

$$\dot{\alpha} = \frac{\dot{n}\, W/S}{\frac{dC_L}{d\alpha} q}$$

and

$$\ddot{\alpha} = \frac{\ddot{n}\, W/S}{\frac{dC_L}{d\alpha} q}$$

The following relation also exists between Δn and $\dot{\gamma}$:

$$\Delta n\, g = \dot{\gamma} V \tag{7}$$

so that

$$\ddot{\gamma} = \frac{\dot{n} g}{V} \tag{8}$$

When equations (6) to (8) are substituted into equations (4) and (5), the four tail-load components then become

$$\Delta L_{t_\alpha} = \frac{dC_m}{dC_L} \frac{WS}{bx_t} \Delta n \tag{9a}$$

$$\Delta L_{t_{\ddot{\alpha}}} = - \frac{W^2 k_Y^2}{gSqx_t \frac{dC_L}{d\alpha}} \ddot{n} \tag{9b}$$

$$\Delta L_{t_{\ddot{\gamma}}} = - \frac{W k_Y^2}{V x_t} \dot{n} \tag{9c}$$

$$\Delta L_{t_c} = \frac{dC_{m_t}}{d\delta} \eta_t q \frac{S_t^2}{b_t x_t} \Delta\delta \tag{9d}$$

Thus, if the variation of the load factor with time Δn and the geometric and aerodynamic characteristics of the airplane were known, the first three components of the tail load could be found immediately. The magnitude of the fourth component, that due to horizontal-tail camber, would follow from equation (3) in which the elevator angle is seen to be

$$\Delta\delta = \frac{\ddot{\alpha}}{K_3} + \frac{K_1}{K_3} \dot{\alpha} + \frac{K_2}{K_3} \Delta\alpha \tag{10}$$

Substitution into equation (10) of the values of $\Delta\alpha$, $\dot{\alpha}$, and $\ddot{\alpha}$ from equation (6) yields the value of the elevator angle at any instant

$$\Delta\delta = \frac{W/S}{K_3 \frac{dC_L}{d\alpha} q}\left(\ddot{n} + K_1\dot{n} + K_2\,\Delta n\right) \tag{11}$$

so that, finally, the fourth component is given as

$$\Delta L_{t_c} = \frac{dC_{m_t}}{d\delta}\,\eta_t\,\frac{S_t^2}{b_t x_t}\,\frac{W/S}{\frac{dC_L}{d\alpha} K_3}\left(\ddot{n} + K_1\dot{n} + K_2\,\Delta n\right) \tag{12}$$

The procedure outlined shows that the tail-load magnitude can be determined if the load-factor variation is known.

Types of load-factor variation.— The relation between the tail load, the geometric and aerodynamic characteristics, and the load factor having been established, it is desirable to establish a load-factor variation which is reasonable as well as critical insofar as loads are concerned. The maximum value of load factor is usually specified; however, there are many possible variations for the shape. Regardless of the details of shape, the load factor may be considered to rise smoothly and continuously to a maximum, the rate of rise depending upon several variables. Beyond the maximum value of the load factor the return to initial conditions can, at the will of the pilot, be either gradual or rapid.

Experiments as well as theoretical studies have already indicated that the maneuver that combines maximum angular and linear accelerations causes critical loads in both the wing and tail. One such maneuver occurs when the maximum load factor is reached as rapidly as possible by using an initial elevator movement which is greater than that required to reach a given steady-trim value of the load factor. This initial elevator movement is followed by a rapid checking of the maneuver either by returning the elevator quickly to neutral or by reversing the controls.

The shape of the load-factor curve for such a maneuver may be expressed approximately by several analytic functions, one of which is

$$\Delta n = a t^b e^{-ct} \tag{13}$$

By way of illustration, figure 2 shows details of the shape of the load-factor curve obtained with the use of equation (13) for which the constants have been adjusted so that an 8g peak is reached in 1 second. By further

adjustment of the constants the load factor can, within certain limits, be made to rise to any specified peak and to diminish in any prescribed manner.

Because the positive slopes obtained from equation (13) are always greater than the negative slopes, the positive angular accelerations are greater than the negative ones. In general, this condition is true for most high g critical maneuvers performed by most classes of airplanes, but maneuvers may occasionally be performed for which the reverse may be true, particularly for small airplanes.

Determination of constants.- From equations (9), (11), and (12) the required quantities relating to load factor are seen to be Δn, $\dot{n}$, and $\ddot{n}$. Since the increment Δn is to be given by

$$\Delta n = at^b e^{-ct} \tag{13}$$

then at maximum load factor

$$\dot{n} = 0 = \Delta n\left(\frac{b}{t} - c\right) \tag{14}$$

Thus $t = \frac{b}{c}$ at maximum load factor. Let $N = \Delta n_{max}$. Then

$$N = a\left(\frac{b}{c}\right)^b e^{-b} \tag{15}$$

so that

$$\frac{\Delta n}{N} = \left(\frac{t}{b/c}\right)^b e^{(b-ct)} \tag{16}$$

Let $\frac{b}{c} = \lambda$. Then

$$\frac{\Delta n}{N} = \left(\frac{t}{\lambda}\right)^b e^{b\left(1-\frac{t}{\lambda}\right)} \tag{17}$$

Equation (17) is in nondimensional form where λ is the time to reach the peak load factor and b is a constant.

When equation (17) is differentiated, the first and second derivatives become

$$\frac{\dot{n}\lambda}{N} = \frac{\Delta n}{N} b\left(\frac{1}{t/\lambda} - 1\right) \tag{18}$$

and

$$\frac{\ddot{n}\lambda^2}{N} = \frac{\Delta n}{N} b^2\left[\frac{\lambda^2}{t^2}\left(1 - \frac{1}{b}\right) - \frac{2\lambda}{t} + 1\right] \tag{19}$$

In equations (17) to (19) the quantities N, λ, and b are now required in order to determine the variation of Δn, $\dot{n}$, and $\ddot{n}$. The value of N is immediately available from the required maneuver load factor, whereas the time to reach the peak load factor λ can be obtained from examination of available records or by specification. The constant b, as may be seen from equation (17), can best be described as a "shape" factor and has no particular physical significance.

The values of λ and b should be associated with a maneuver which produces maximum tail loads. Therefore the time λ to reach peak load factor should be the minimum possible consistent with possible pilot action and airplane response. The shape factor b should also be consistent with both of these.

In connection with the determination of the minimum time to reach peak load factor, the results shown in figure 3 for a typical airplane are informative. Figure 3(a) shows the load-factor variation following several abrupt jump elevator movements. The load factor varies with the elevator position, but the time to reach peak load factor does not. Figure 3(b) shows the load-factor variation for several abrupt hat-shape elevator impulses. Again the load factor is seen to vary with the amount of elevator deflection but the time to reach the peak value remains constant. Although the time to reach the peak load factor shown in figure 3(b) remains constant, it is seen to be less than that shown in the previous case; therefore, an impulse elevator motion produces a smaller value of λ than the jump type.

Because of inertia and elasticity in the control system, the pilot cannot move the elevator instantaneously but requires some finite time t_1 to do so. A possible critical type of elevator impulse thus appears to be one which increases linearly to maximum and decreases at the same rate to zero. In order to determine the minimum time to reach peak load factor associated with such a variation, the equation of motion (equation (3)) has been solved for the triangular elevator impulse for airplanes of various static stabilities and damping.

The results of the computations are given in figure 4 in which the minimum time λ to reach peak load factor is plotted against the time t_1 required to deflect the elevator.

For completeness the curves of figure 4 are labeled for the actual values of K_2 employed in the computation as well as for relative values of stability. By a series of computations the damping term K_1 was found, as was to be expected, to have only a secondary effect on λ. The curves apply to an average value of the damping constant. The upper curve, labeled "low stability," should be associated with rearward center-of-gravity positions (that is, low static margin) in combination with one or both of the following: low dynamic pressure or heavy airplanes. The lower curve, labeled "high stability," would be associated with forward center-of-gravity positions in combination with one or both of the following: high dynamic pressure or light airplanes. It is seen that λ increases almost linearly with t_1 and also increases when the restoring forces are reduced, that is, when the stability is reduced.

A preliminary value of the shape factor b (required in equations (17) to (19)) was initially determined from flight records of typical impulse maneuvers by fitting curves of the type given by equation (13) through several points of the actual time histories and determining the constants. The results of this first step were then modified by the results of the same computations which had been made to determine λ, and the variation of b with t_1 given in figure 5 was obtained. Since the b factor is not found to be critical, an average value of 5.0 is suggested, although as a refinement the values from figure 5 may be used.

The question of the value of t_1 to use is one which must be solved either from experience or from a knowledge of the characteristics of the controls and the control system. For conventional airplanes having the usual amounts of boost and no rate restrictors, the following values of t_1 are suggested as representative:

	t_1
Fighters or small civil airplanes with weight limit from about 500 to 12,000 pounds, seconds	0.20
Two-engine airplanes with weight limit from 25,000 to 45,000 pounds, seconds	0.25
Four-engine airplanes with weight limit from 50,000 to 80,000 pounds, seconds	0.30
Airplanes with weight limit above 100,000 pounds, seconds	0.40

The minimum time λ given in figure 4 was actually established separately from the adopted load-factor variation; therefore, in applying the inverse method, the derived elevator impulse would not be expected to agree in detail with the "tent" type impulse used in the derivation.

The first three tail-load components can now be computed by inserting the values of Δn, $\dot{n}$, and $\ddot{n}$ from equations (17) to (19) into equation (9) and using appropriate values of λ from figure 4. In order to facilitate this computation, curves of $\Delta n/N$, $\dot{n}\lambda/N$, and $\ddot{n}\lambda^2/N$ plotted against t/λ are given in figure 6 for the suggested value of $b = 5$. Actually to apply the results of figure 6 it is convenient to find first the components ΔL_{t_α}, and so forth, in terms of the nondimensional time t/λ and then to convert to time t in seconds. In order either to compute the fourth component or to obtain the elevator angles for use in chord loading, the constants K_1, K_2, and K_3 of equation (3) must also be known.

Thus, in terms of t/λ and the ordinates of figure 6, the various tail-load components are

$$\Delta L_{t_\alpha} = \frac{dC_m}{dC_L}\frac{WSN}{bx_t}\left(\text{Ordinate of fig. 6(a)}\right) \tag{20a}$$

$$\Delta L_{t_{\ddot{\alpha}}} = \frac{-W^2k_Y^2}{gSqx_t\dfrac{dC_L}{d\alpha}}\frac{N}{\lambda^2}\left(\text{Ordinate of fig. 6(c)}\right) \tag{20b}$$

$$\Delta L_{t_{\ddot{\gamma}}} = \frac{-Wk_Y^2}{Vx_t}\frac{N}{\lambda}\left(\text{Ordinate of fig. 6(b)}\right) \tag{20c}$$

$$\Delta L_{t_c} = \frac{dC_{m_t}}{d\delta}\eta_t\frac{S_t^2}{b_tx_t}\frac{W}{S}\frac{N}{K_3\dfrac{dC_L}{d\alpha}}\left[\frac{\text{Ordinate of fig. 6(c)}}{\lambda^2} + \frac{K_1\left(\text{Ordinate of fig. 6(b)}\right)}{\lambda} + K_2\left(\text{Ordinate of fig. 6(a)}\right)\right] \tag{20d}$$

The constants K_1, K_2, and K_3 defined in table I are the same as those given in reference 2, except for changed signs caused by specifying x_t as positive.

The conversion to time t is made by multiplying values of the base scale t/λ by λ.

Sample calculations for incremental tail loads.- The results of several examples are given to illustrate not only the method but also the effect of each of a number of variables on the incremental tail load of a typical fighter airplane, the geometric and aerodynamic characteristics of which are given in the following tables. In order to illustrate the effect of static stability, results have been computed for three center-of-gravity positions with the assumption that an 8g recovery is made at 19,100 feet from a vertical dive at an equivalent airspeed of 400 miles per hour. In order to illustrate the effect of the time of the elevator impulse on the tail load, computations were carried out at one of the center-of-gravity positions for several values of t_1. The cases considered and the airplane characteristics follow:

GEOMETRIC CHARACTERISTICS

Gross wing area, S, square feet	300
Gross horizontal-tail area, S_t, square feet	60
Airplane weight, W, pounds	12,000
Wing span, b, feet	41
Tail span, b_t, feet	16
Radius of gyration, k_Y, feet	6.4
Distance from aerodynamic center of airplane less tail to aerodynamic center of tail, x_t, feet:	
Center of gravity, 29 percent M.A.C.	20.0
Center of gravity, 24 percent M.A.C.	20.3
Center of gravity at aerodynamic center	21.0

AERODYNAMIC CHARACTERISTICS

Slope of airplane lift curve, $dC_L/d\alpha$, radians	4.87
Slope of tail lift curve, $dC_{L_t}/d\alpha_t$, radians	3.15
Downwash factor, $d\epsilon/d\alpha$	0.54
Tail efficiency factor (q_t/q), η_t	1.00
Empirical airplane damping factor, K	1.1
Elevator effectiveness factor, $dC_{L_t}/d\delta$, radians	1.89
Rate of change of tail moment with camber due to elevator angle, $dC_{m_t}/d\delta$, radian	-0.57

Rate of change of moment coefficient with angle of attack for airplane less tail, $dC_m/d\alpha$, radians:

Center of gravity, 29 percent M.A.C.	0.625
Center of gravity, 24 percent M.A.C.	0.403
Center of gravity at aerodynamic center	0.000

The specified conditions for the sample computations are given in table II. The computed results for tail components are given in figures 7 and 8. Figure 7 gives results for varying the center of gravity and figure 8 gives similar results for varying t_1. The tail-load components are computed from equations (20) and the derived elevator angles from equation (11). If the increment in tail load due to camber and the incremental elevator angle are not required, the K values need not be computed and the computations are considerably shortened. Figures 7 and 8 show that a maximum error of only about 4 percent is introduced by this omission.

Method of Determining the Total Tail Load

The initial or steady-flight tail load and elevator angles to which the computed incremental values are to be added must also be determined. In steady flight, the horizontal tail furnishes the moment required to balance the moments from all other parts of the airplane so that the initial load may be written as

$$L_{t_o} = \frac{C_{m_o} qSc}{x_t} + \frac{dC_m}{dC_L} \frac{WS}{bx_t} \cos \gamma_o \qquad (21)$$

Thus the total tail load at any time in a maneuver is composed of the four previously mentioned parts plus the components given in equation (21). Only the first term of equation (21) represents a new type of load because the second term is a load of the type given by equation (9a) or equation (20a) and its effect may be immediately included in the computations by multiplying the ordinates of figure 6 by $N + \cos \gamma_o$ instead of by N.

The initial elevator angle required to balance the airplane in steady flight varies with airplane C_L and center-of-gravity position so that, in general, δ_o must be obtained from wind-tunnel data. Without results of wind-tunnel tests, a rough rule which can be used as a guide at the design stage in determining the elevator position is that

the final elevator setting will be so adjusted by repositioning of the stabilizer setting during acceptance tests that it will be near a zero position at the cruising speed and at the most prevalent center-of-gravity position.

Method of Determining Maximum Values

Maximum tail loads and angular accelerations.- The method outlined enables a point-by-point evaluation to be made of the quantities that determine the tail load. Such detail may often be unnecessary and the procedure may be shortened by evaluating only those points near the load peaks or, alternatively, by accepting an approximation to the results. One such approximation which may be made is to balance the airplane at the combinations of load factor and angular acceleration which would result in maximum up and down tail loads.

Figure 7 shows that the maximum down tail load in a pull-up occurs near the start of the maneuver and before appreciable load factor is reached. This maximum load is practically coincident with the negative maximum in the $L_{t_{\ddot{\alpha}}}$ tail-load component. Since, for a given configuration, this component increases as the center of gravity is moved forward and since the steady-flight down load increases with speed, the maximum down tail load in a pull-up occurs at the highest design speed in combination with the most forward center-of-gravity position.

Figures 7 and 8 show that at the time of the maximum down-tail-load increment the elevator is near but has not quite reached its peak position. Also at the time of maximum up-tail-load increment the elevator is near its zero position, although it may be on either side of this position depending upon the stability and the time t_1. These results suggest that the maximum down load for the elevator and the hinge brackets would occur with the airplane center of gravity well forward and at the start of the maneuver. The maximum load for the stabilizer is likely to occur at the peak load factor.

Figure 7 also shows that the up tail load occurs near the peak of the $L_{t_{\alpha}}$ component as well as near the positive maximum peak in the $L_{t_{\ddot{\alpha}}}$ component. Since the $L_{t_{\alpha}}$ component increases as the center of gravity is moved rearward and since a decrease in speed generally reduces the initial down load, the maximum up tail load occurs at the upper left-hand corner of the V-n diagram for the most rearward center-of-gravity position.

The maximum tail load in a pull-up maneuver may be written as

$$L_{t_{max}} = \frac{C_{m_o} qSc}{x_t} + \frac{dC_m}{dC_L} \frac{WS}{bx_t} (n + \cos \gamma_o) - \frac{I\ddot{\theta}}{x_t} \qquad (22)$$

where the sum of the second and third terms is to be a maximum in the maneuver. From the previous discussion the load-factor increment at maximum down load is nearly zero and at maximum up load it is nearly equal to N so that if the positive and negative values of $\ddot{\theta}_{max}$ can be determined, a relatively simple method for determining maximum loads is available.

Since by definition $\ddot{\theta} = \ddot{\alpha} + \ddot{\gamma}$, an expression for angular acceleration can be derived from equations (6) and (7) and written in the form

$$\ddot{\theta} = \frac{W/S}{C_{L_\alpha} q} \ddot{n} + \frac{g}{V} \dot{n}$$

The maximum angular acceleration can be approximated by

$$\ddot{\theta}_{max} = B \frac{W/S}{\frac{dC_L}{d\alpha} q} \frac{N}{\lambda^2} + C \frac{gN}{V\lambda} \qquad (23)$$

For the maximum positive pitching acceleration, B is the maximum positive ordinate in figure 6(c) and C is the ordinate of figure 6(b) at a value of t/λ for which B was determined. Thus, B is 6.5 and C is 0.95 for this example.

For the maximum negative pitching acceleration, B is the maximum negative ordinate in figure 6(c) and C is the ordinate of figure 6(b) at a value of t/λ for which B was determined. Thus, B is -5.8 and C is 0.80. For use in equation (23) the values of λ for the maneuver are available from figure 4 and the other quantities are available from the conditions of the problem. The maximum loads can be given by the following equations:

For maximum up tail load in the pull-up:

$$L_{t_{max+}} = \frac{C_{m_o} qSc}{x_t} + \frac{dC_m}{dC_L} \frac{WS}{bx_t} (N + 1.0) + \frac{I_Y}{x_t} \frac{N}{\lambda} \left(\frac{5.8\ W/S}{\frac{dC_L}{d\alpha} q\lambda} - \frac{0.8g}{V} \right) \quad (24a)$$

For maximum down tail load in the pull-up:

$$L_{t_{max-}} = \frac{C_{m_o} qSc}{x_t} + \frac{dC_m}{dC_L} \frac{WS}{bx_t} \cos \gamma - \frac{I_Y}{x_t} \frac{N}{\lambda} \left(\frac{6.5\ W/S}{\frac{dC_L}{d\alpha} q\lambda} + \frac{0.95g}{V} \right) \quad (24b)$$

For push-downs to limit load factor, equations (24a) and (24b) still apply with changed signs for N and changed directions for $L_{t_{max+}}$ and $L_{t_{max-}}$. A question arises as to whether the maximum down tail load at the start of a pull-up with forward center-of-gravity position is greater than that which would occur when pulling up from a negative load-factor condition, with the center of gravity in the most rearward position. This can be determined only by computing both cases and seeing which is the larger.

Maximum value of angular velocity.- The maximum value of the pitching angular velocity in the pull-up may also be found in a manner similar to that used to obtain the maximum angular acceleration. Since $\dot{\theta} = \dot{\alpha} + \dot{\gamma}$ and the relations involving these quantities in terms of load factor are given by equations (6) and (7), the following equation may be written:

$$\dot{\theta} = \frac{\dot{n}\ W/S}{\frac{dC_L}{d\alpha} q} + \frac{\Delta n\ g}{V} \quad (25)$$

The maximum angular velocity may be approximated by

$$\dot{\theta} = D \frac{N}{\lambda} \frac{W/S}{\frac{dC_L}{d\alpha} q} + E \frac{Ng}{V} \quad (26)$$

where D is the maximum positive ordinate in figure 6(b) and E is the ordinate of figure 6(a) at a value of t/λ for which D was determined. Thus D, for this example, is 1.95 and E is 0.48.

In the steady turn or pull-up at constant g, the angular velocity is usually given by the expression $\dot{\theta} = 1.0 \frac{gN}{V}$. The difference between the factor 1.0 of this expression and the factor 0.48 of equation (26) is more than made up by the angle-of-attack component of the angular velocity.

Approximate Method of Determining Load Distribution

Symmetrical loading.— The spanwise distribution of the total load can be formulated with various degrees of exactness. If information regarding details of the angle-of-attack distribution across the span were available, then an exact solution could be obtained for the loading with the use of existing lifting-surface methods. The following method may be used as a first approximation to the solution.

From the total tail load, the total tail lift coefficient C_{L_t} can readily be found. The average effective angle of attack $\bar{\alpha}$ of the stabilizer portion is given in the definition

$$C_{L_t} = \int_0^1 c_{l_\alpha} \bar{\alpha} \frac{c}{\bar{c}} \, dy^* + \int_0^1 c_{l_\delta} (\delta_o + \Delta\delta) \frac{c}{\bar{c}} \, dy^* \tag{27}$$

where only $\bar{\alpha}$ is assumed as unknown and c_{l_α} and c_{l_δ} may be taken as the rates of change of section lift coefficient with α and δ, respectively.

Thus, for constant elevator angle across the span,

$$\bar{\alpha} = \frac{C_{L_t} - (\delta_o + \Delta\delta) \int_0^1 c_{l_\delta} \frac{c}{\bar{c}} \, dy^*}{\int_0^1 c_{l_\alpha} \frac{c}{\bar{c}} \, dy^*} \tag{28}$$

In a practical case both integrals in equation (28) need be evaluated only once for a given configuration and Mach number. A plot of $\bar{\alpha}$ against C_{L_t} with δ as a parameter would be useful in further computations. With $\bar{\alpha}$ known as a function of C_{L_t} and δ, the local lift at any spanwise station is then obtained from the expression

$$l = c_{l_t} q c = \left[c_{l_\alpha} \bar{\alpha} + c_{l_\delta} (\delta_o + \Delta\delta) \right] q c \tag{29}$$

Unsymmetrical loading.— Up to this point the total loads have been assumed to be symmetrical about the airplane center line, whereas, in reality, the load may have an unsymmetrical part. The sources of this dissymmetry may be due to uneven rigging, differences in elasticity between the two sides, or to effects of slipstream, rolling, and sideslip. The first two sources are usually inadvertent ones while the last two are difficult to determine without either wind-tunnel tests or a knowledge of how the airplane will be operated. Present design rules regarding dissymmetry of tail load are concerned more with providing adequate design conditions for the rear of the fuselage than with recognizing that at the maximum critical tail load some dissymmetry may exist.

Tests in the Langley full-scale tunnel (reference 6) and flight tests (reference 7) of a fighter-type airplane, as well as unpublished flight tests of another fighter-type airplane, indicate that the tail-load dissymmetry varies linearly with angle of sideslip so that the difference in lift coefficient between the two sides of the tail can be given as

$$C_{L_{t_{Right}}} - C_{L_{t_{Left}}} = A\beta \tag{30}$$

The average values of A per degree found for the two fighter-type airplanes are approximately 0.01. No similar values are available for larger airplanes nor for tail surfaces having appreciable dihedral.

In maneuvers of the type considered herein it is doubtful that angles of sideslip larger than 3° would be developed at the time the maximum tail load is reached. If the value of the sideslip angle at the time of maximum tail load can be established, equations (27) to (29) are easily modified to include this effect, provided the approximate value of A is known.

Chordwise loading.- The chordwise distribution can be determined for any one spanwise station in either of two ways. One way for design work is outlined in reference 8. A knowledge of the airfoil section and the quantities contained in equation (29) suffices for this determination.

If pressure-distribution data are available for a similar section with flaps, an alternate way would be to distribute the load chordwise according to the two-dimensional pressure diagrams with the use of the computed values of section lift coefficient and elevator angle.

DISCUSSION

The method presented is another approach to the determination of tail loads. From the results given in figures 7 and 8, it can be seen that the camber component L_{t_c} is so small that for all practical cases it may be omitted with considerable simplification in the computation of tail loads. This omission reduces to a minimum the number of aerodynamic parameters needed to compute the tail loads.

It is possible, in the application of the present method with the use of the suggested values of t_1, that the derived elevator angles may not be within the pilot's capabilities. Since it must be assumed that all airplanes, to be satisfactory, should have sufficient control to reach their design load boundaries, such an occurrence requires only that the time to reach elevator peak deflection t_1 be increased so as to reduce the elevator angle. The results of figure 8, in which the time t_1 is varied, furnish a useful guide for determining the increase t_1 that might be required.

If sufficient information is available, it is recommended that existing lifting-surface methods be used in determining the spanwise distribution of the total load; however, if information of the angle-of-attack distribution across the span is not known, the method presented may be used as a first approximation.

Along some of the boundaries of the V-n diagram, tail buffeting may occur. Measurements show that buffeting usually occurs along the line of maximum lift coefficient and again along a high-speed buffet line which is associated with a compressibility or force break on some major part of the airplane. All airplanes are subject to buffeting at the design conditions associated with the left-hand corner of the V-n diagram.

Only high-speed and/or high-altitude airplanes are capable of reaching the other boundary. Measurements show that the oscillatory buffeting loads may be so high that the designer should at least be cognizant of them at the design stage.

The maximum angular acceleration varies inversely with airspeed and directly with the load factor, with the contribution due to acceleration in angle of attack likely to be more important than the angular acceleration of the flight path. A somewhat similar variation is indicated for the maximum angular velocity (equation (26)) where it is seen by direct substitution that the part due to angle of attack is likely to be larger than the part due to the angular velocity of the flight path.

CONCLUDING REMARKS

A simple method has been presented for determining the horizontal tail loads in maneuvering flight with the use of a prescribed incremental load-factor variation.

The incremental tail load was separated into four components representing α, $\ddot{\alpha}$, $\ddot{\gamma}$, and c. The camber component L_{t_c} is so small that for most conventional airplanes it may be neglected, thereby reducing to a minimum the number of aerodynamic parameters needed in this computation of tail loads.

An approximate method is presented for predicting maximum angular accelerations and maximum angular velocities.

The method indicates that maximum tail loads in a pull-up occur at forward center-of-gravity positions and early in the maneuver. The maximum down tail loads in a pull-up occur at the highest design speed in combination with the most forward center-of-gravity position. The maximum up tail load occurs at the upper left-hand corner of the V-n diagram for the most rearward center-of-gravity positions.

Langley Aeronautical Laboratory
National Advisory Committee for Aeronautics
Langley Air Force Base, Va., February 9, 1950

REFERENCES

1. Schmidt, W., and Clasen, R.: Luftkräfte auf Flügel und Höhenleitwerk bei einem Höhenruderausschlag $\beta_H = \beta_{H_{max}} \cdot kte^{1-kt}$ im waagerechten Geradeausflug. Jahrb. 1937 der deutschen Luftfahrtforschung, R. Oldenbourg (Munich), pp. I 169 – I 173.

2. Pearson, Henry A.: Derivation of Charts for Determining the Horizontal Tail Load Variation with Any Elevator Motion. NACA Rep. 759, 1943.

3. Kelley, Joseph, Jr., and Missall, John W.: Maneuvering Horizontal Tail Loads. AAF TR No. 5185, Air Technical Service Command, Army Air Forces, Jan. 25, 1945.

4. Dickinson, H. B.: Maneuverability and Control Surface Strength Criteria for Large Airplanes. Jour. Aero. Sci., vol. 7, no. 11, Sept. 1940, pp. 469–477.

5. Matheny, Cloyce E.: Comparison between Calculated and Measured Loads on Wing and Horizontal Tail in Pull-Up Maneuvers. NACA ARR L5H11, 1945.

6. Sweberg, Harold H., and Dingeldein, Richard C.: Effects of Propeller Operation and Angle of Yaw on the Distribution of the Load on the Horizontal Tail Surface of a Typical Pursuit Airplane. NACA ARR 4B10, 1944.

7. Garvin, John B.: Flight Measurements of Aerodynamic Loads on the Horizontal Tail Surface of a Fighter-Type Airplane. NACA TN 1483, 1947.

8. Anon.: Chordwise Air-Load Distribution. ANC-1(2), Army-Navy-Civil Committee on Aircraft Design Criteria, Oct. 28, 1942.

TABLE I

CONSTANTS OCCURRING IN BASIC DIFFERENTIAL EQUATION

Constant	Definition
K_1	$\frac{\rho V}{2m}\left[\frac{dC_{L_t}}{d\alpha_t}\frac{S_t x_t^2}{k_Y^2}\eta_t\left(\frac{K}{\sqrt{\eta_t}}+\frac{d\epsilon}{d\alpha}\right)+\frac{dC_L}{d\alpha}S\right]$
K_2	$-\frac{\rho V^2}{2m}\left\{\frac{dC_m}{d\alpha}\frac{S^2}{k_Y^2 b}-\frac{dC_{L_t}}{d\alpha_t}\eta_t\frac{S_t x_t}{k_Y^2}\left[\left(1-\frac{d\epsilon}{d\alpha}\right)+\frac{dC_L}{d\alpha}\frac{K}{\sqrt{\eta_t}}\frac{\rho}{2}\frac{Sx_t}{m}\right]\right\}$
K_3	$\frac{\rho V^2}{2m}\left(-\frac{dC_{L_t}}{d\delta}\eta_t\frac{S_t x_t}{k_Y^2}+\frac{dC_{m_t}}{d\delta}\eta_t\frac{S_t^2}{b_t k_Y^2}-\frac{dC_{L_t}}{d\alpha_t}\frac{dC_{L_t}}{d\delta}\frac{K\eta_t^2}{\sqrt{\eta_t}}\frac{\rho}{2}\frac{x_t^2 S_t^2}{mk_Y^2}\right)$

TABLE II

SPECIFIED CONDITIONS OF SAMPLE PROBLEM

Increment in load factor	8.0
Altitude, feet	19,100
Air density, slug per cubic foot	0.001306

Case	cg (percent M.A.C.)	t_1	K_1	K_2	K_3	λ (fig. 4)
1	a.c.	0.2	4.93	30.4	−33.4	0.45
2	24	.2	4.72	16.2	−32.2	.50
3	29	.2	4.61	8.45	−31.7	.56
4	24	.4	4.72	16.2	−32.2	.77
5	24	.6	4.72	16.2	−32.2	1.02

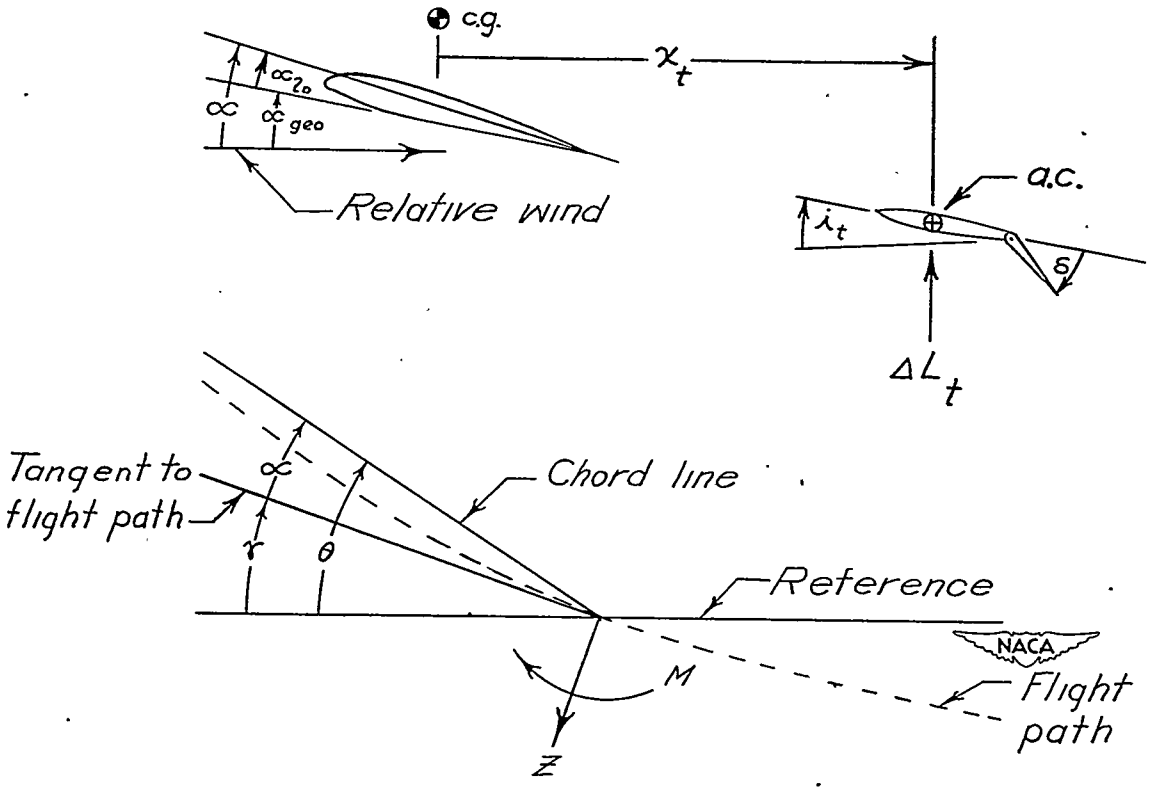

Figure 1.- Sign conventions employed. Positive directions shown.

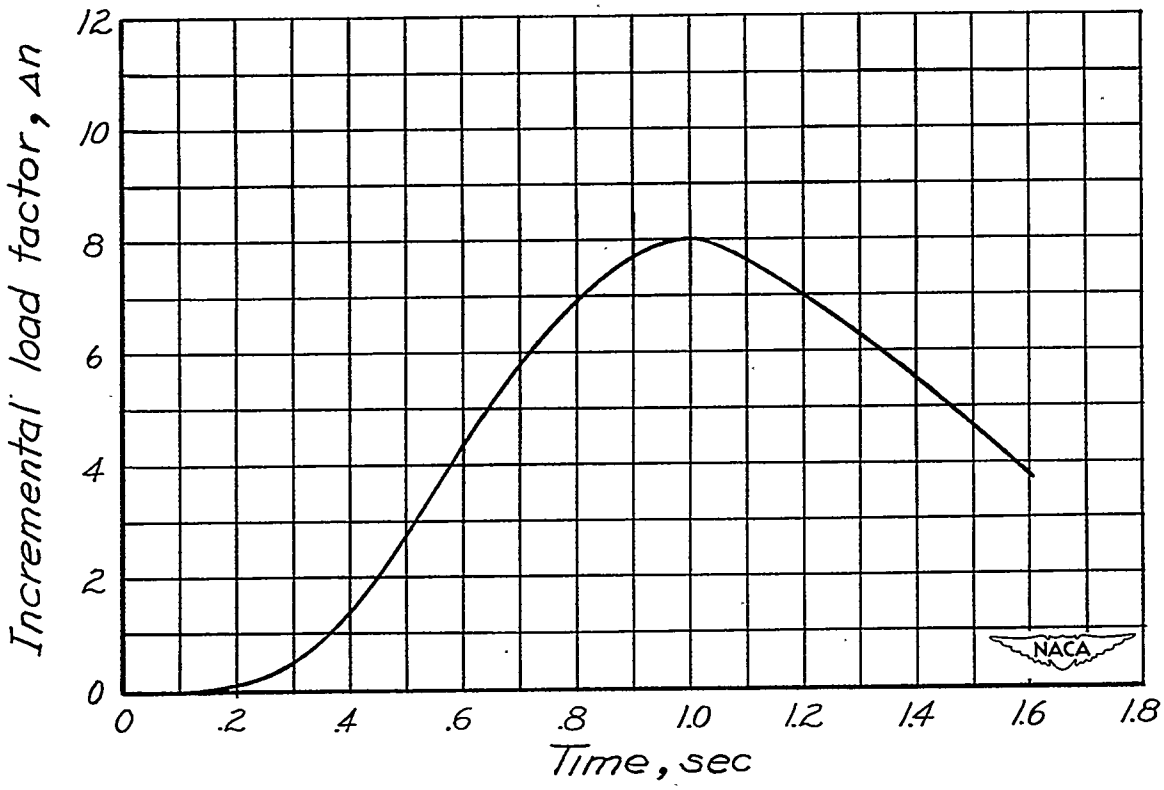

Figure 2.- Variation of load-factor increment. $\Delta n = N250t^{5.53}e^{-5.53}$.

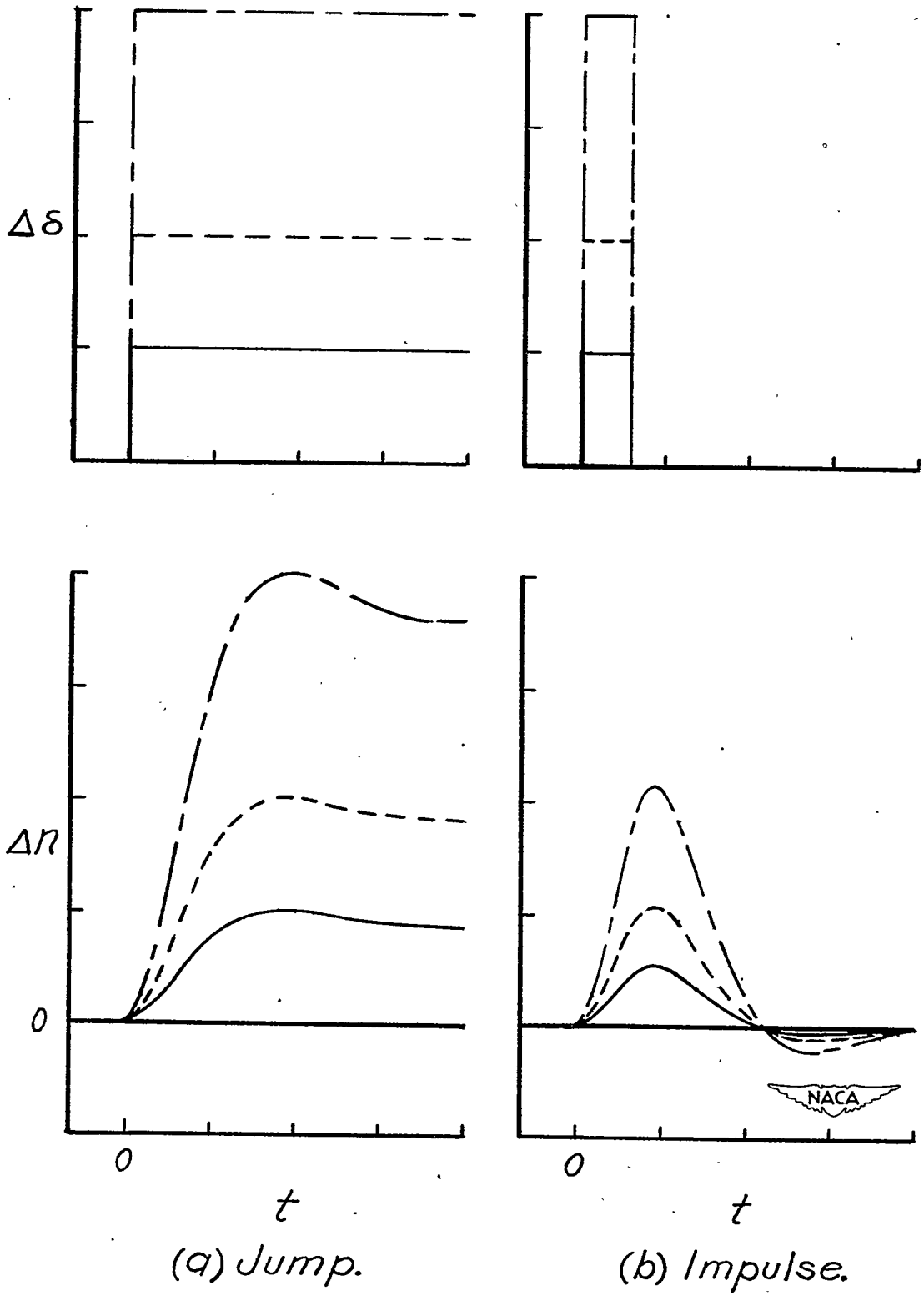

Figure 3.- Incremental-load-factor variations following control movement.

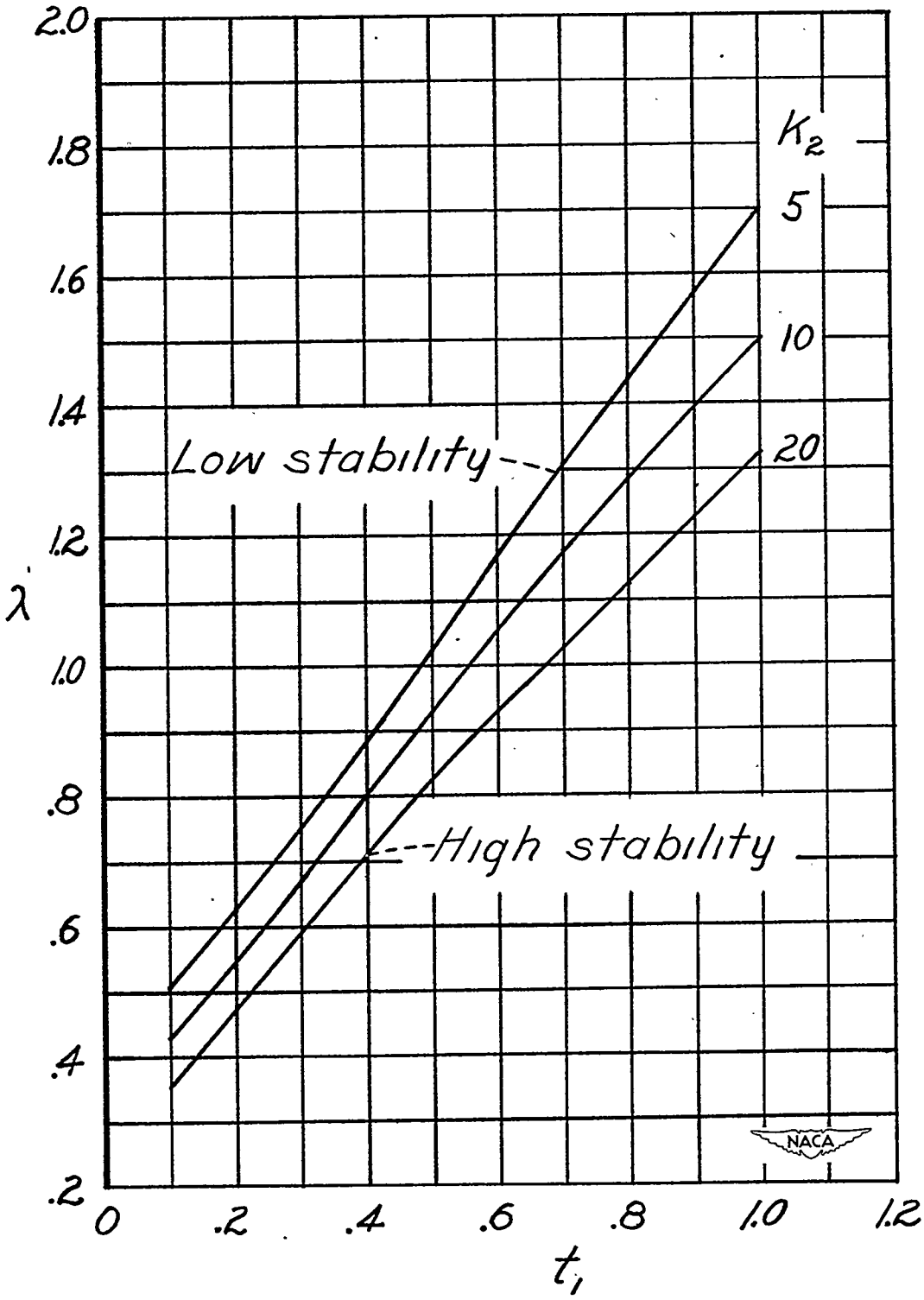

Figure 4.- Variation of λ with t_1.

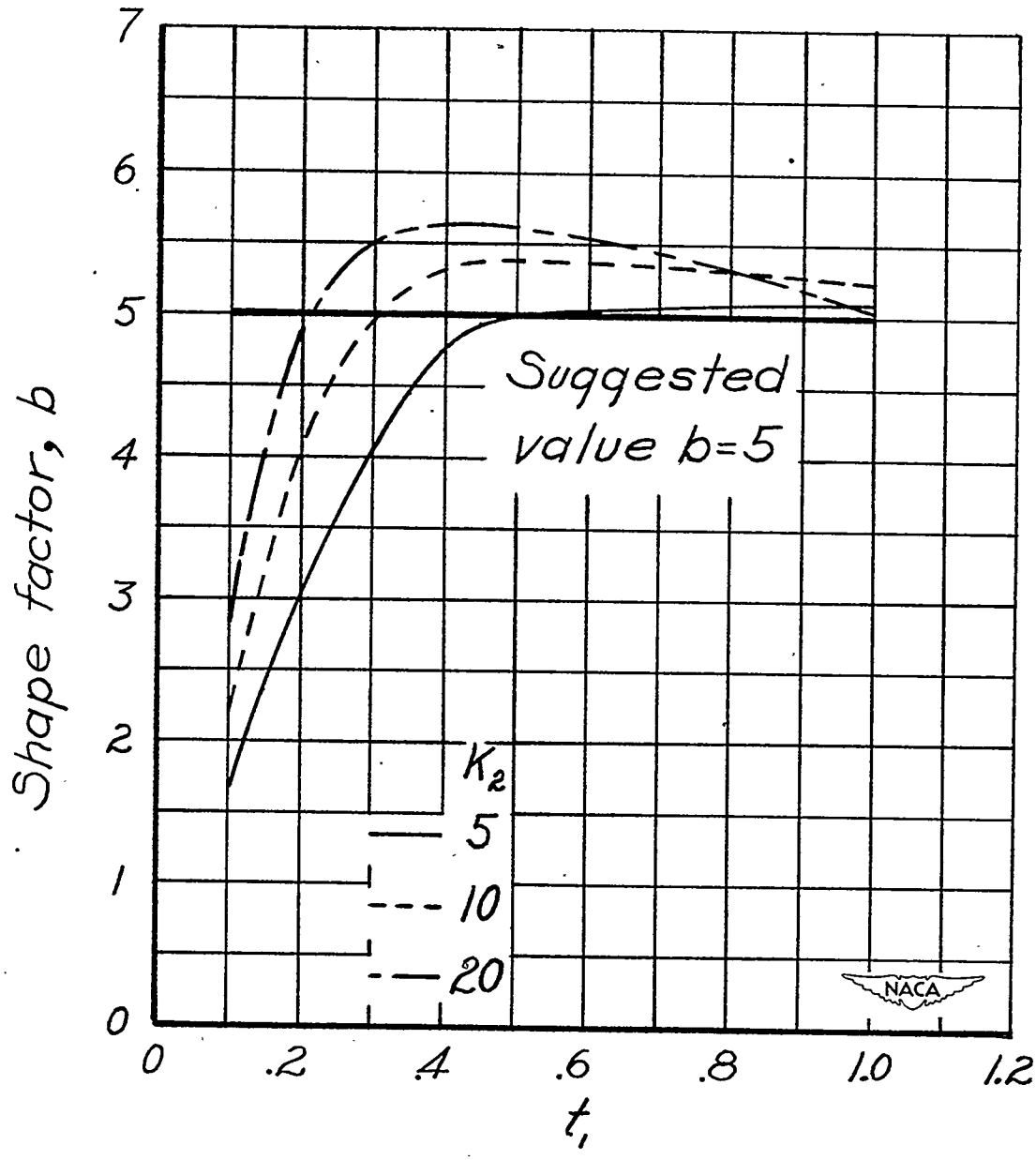

Figure 5.- Variation of shape factor b with t_1.

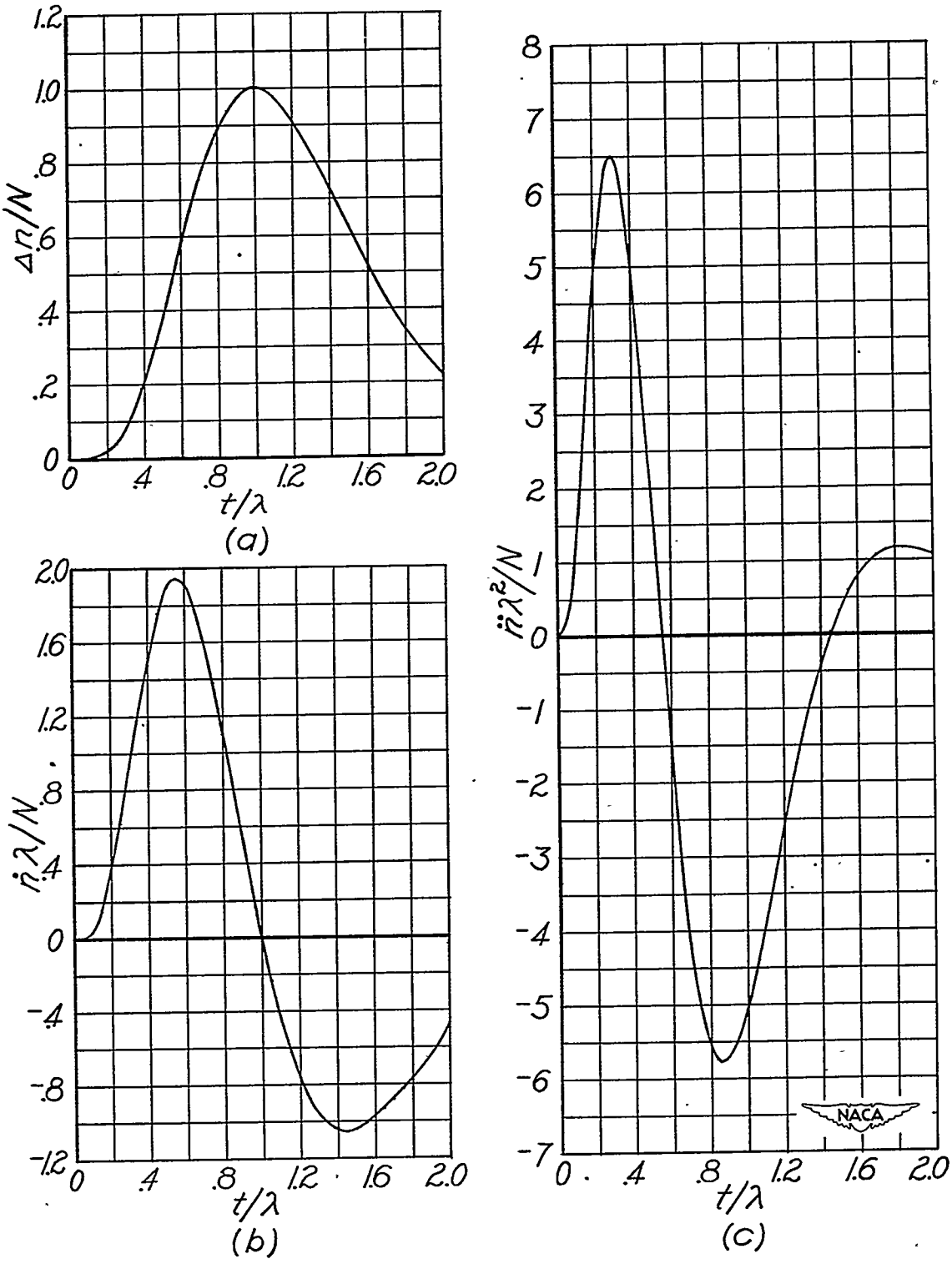

Figure 6.- Variation of incremental-load-factor curves with time ratio.

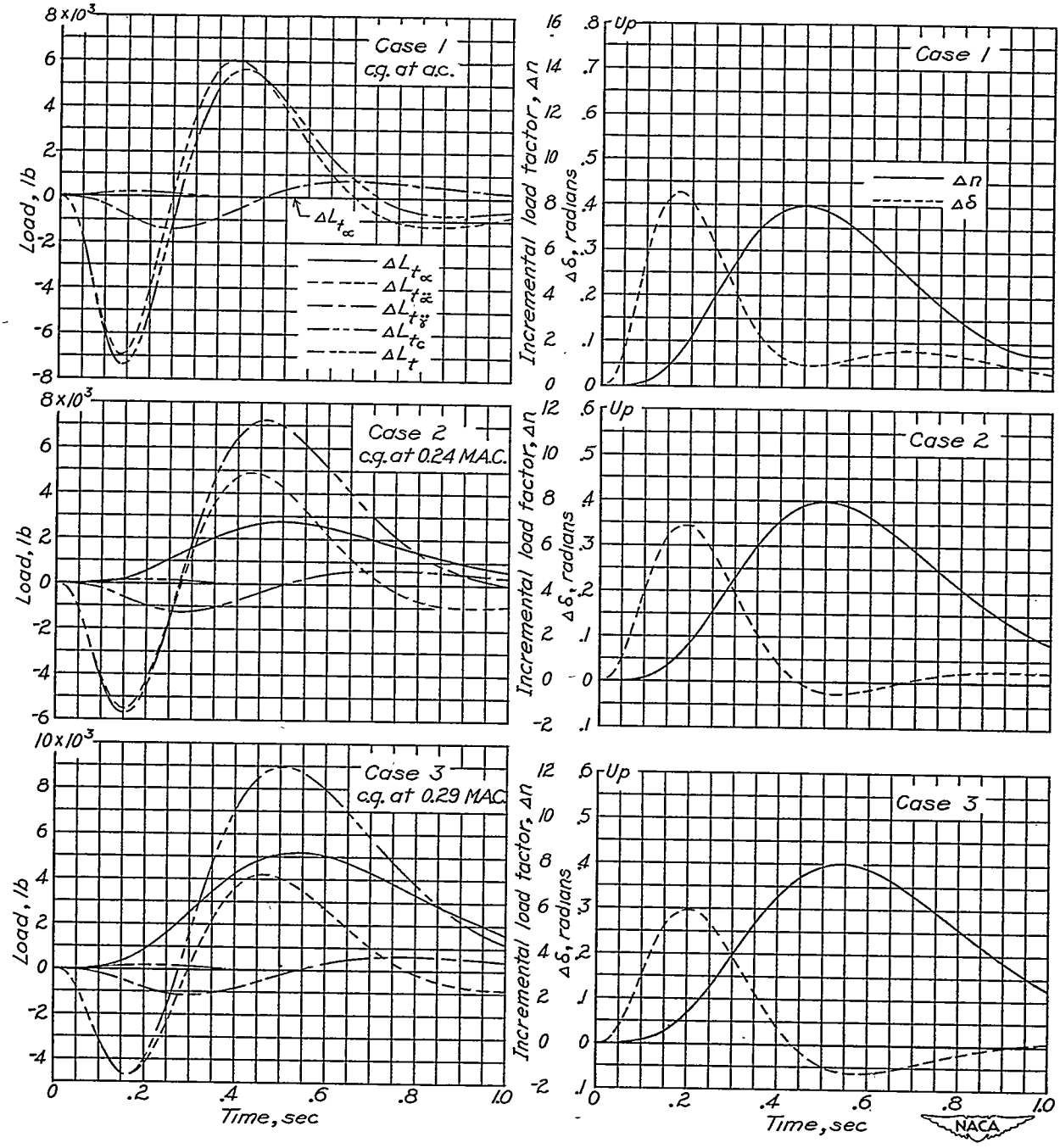

Figure 7.- Effect of center-of-gravity position on incremental-tail-load components.

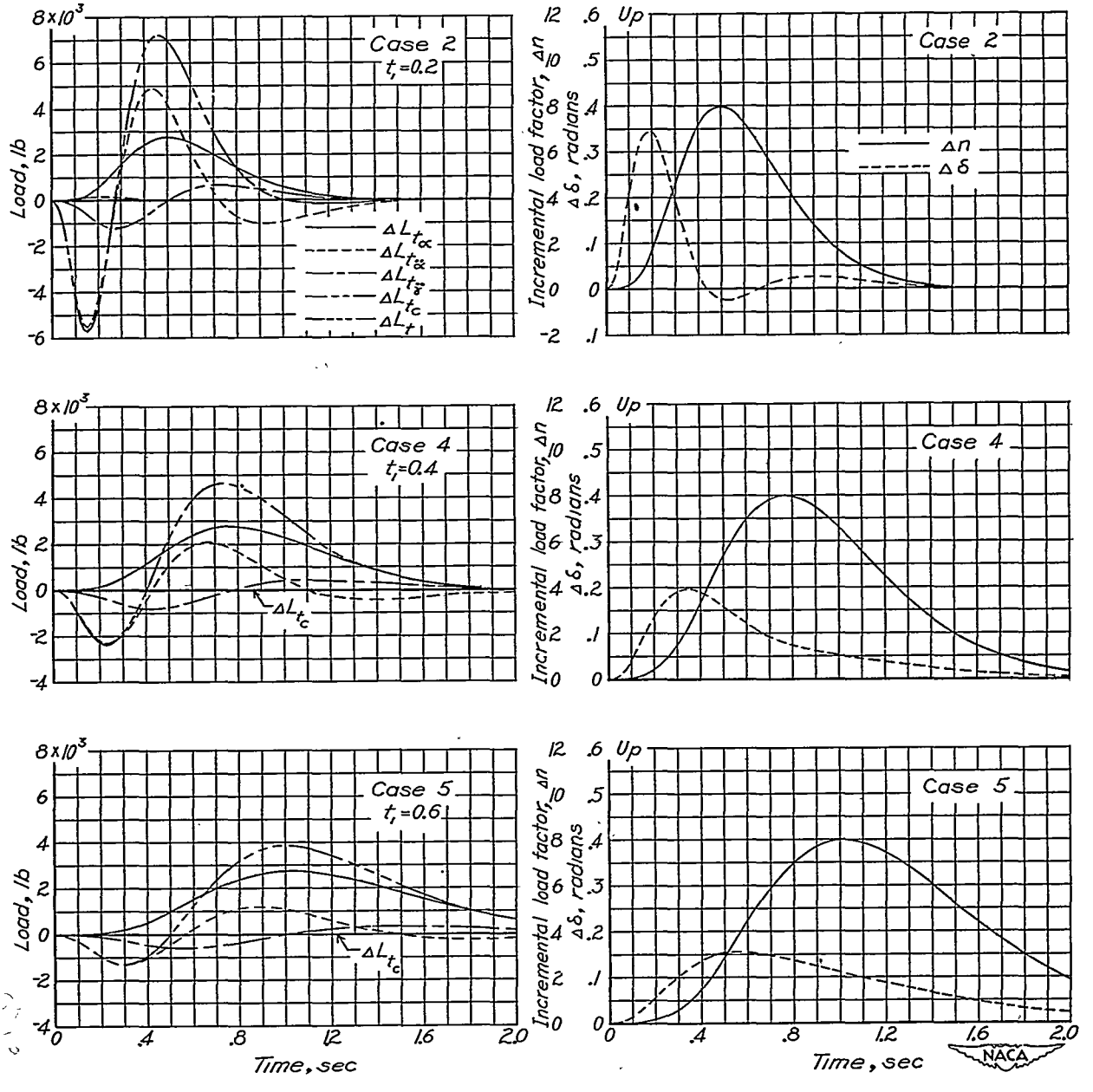

Figure 8.- Effect of t_1 on incremental-tail-load components. Center of gravity, 0.24 $\bar{c}$.